

Autonomous Driving among Many Pedestrians: Models and Algorithms

Yuanfu Luo¹ Panpan Cai¹ Aniket Bera² David Hsu¹ Wee Sun Lee¹ Dinesh Manocha²

Abstract—Driving among a dense crowd of pedestrians is a major challenge for autonomous vehicles. This paper presents a planning system for autonomous driving among many pedestrians. A key ingredient of our approach is a pedestrian motion prediction model that accounts for both a pedestrian’s global navigation intention and local interactions with the vehicle and other pedestrians. Unfortunately, the autonomous vehicle does not know the pedestrian’s intention a priori and requires a planning algorithm that hedges against the uncertainty in pedestrian intentions. Our planning system combines a POMDP algorithm with the pedestrian motion model and runs in near real time. Experiments show that it enables a robot vehicle to drive safely, efficiently, and smoothly among a crowd with a density of nearly one person per square meter.

I. INTRODUCTION

Autonomous driving among pedestrians is a key ability of many autonomous robots, such as rescue robots in disasters, and assistive robots in public places like hospitals, airport terminals, etc. The main concerns in these applications are safety, efficiency and smoothness of the driving. Driving among many pedestrians is challenging because of the uncertain motion of pedestrians, imperfect control of the robot, sensor noises, environment changes, etc.

To pursue a successful drive, a robot vehicle must predict the motions of the surrounding pedestrians. Pedestrians’ motions are typically guided by their *intentions* and *interactions*. Intentions are pedestrians’ long-term navigation goals; pedestrians’ interactions, often guided by their intentions, are short-term reactions to obstructions such as vehicles and other pedestrians. A pedestrian motion model need to consider both intentions and interactions to achieve accurate predictions. Otherwise, it may predict completely wrong moving directions, or generate infeasible motions such as penetrating obstacles.

Integrating an accurate pedestrian motion model enables a planning algorithm to drive a vehicle safely, efficiently, and smoothly. Unfortunately, pedestrians’ intentions and interactions contain significant uncertainty: intentions of pedestrians are not directly observable to the vehicle; their interactions also subject to noises due to individual difference such as age, gender, etc. Handling the uncertainty is essential for robust planning.

Our planning system incorporates pedestrian intentions, interactions, and their uncertainty in a principled manner. We first develop a pedestrian motion model that incorporates both intentions and interactions. We then integrate

the model with a Partially Observable Markov Decision Process (POMDP) to plan for optimal vehicle control under uncertainty.

Our pedestrian motion model is based on Optimal Reciprocal Collision Avoidance (ORCA) [1]. ORCA predicts pedestrian motions by considering their *reciprocal collision avoidance*. We improve ORCA in two ways. First, we introduce pedestrian-vehicle interactions into the model, by considering the non-holonomic nature of the robot vehicle that forbids side-wise movement. Second, we correct the greedy behaviors of simulated pedestrians in ORCA. This greediness causes a *freezing pedestrian problem* when simulated pedestrians encounter obstacles in front: they often walk very slowly or even stay stationary, instead of making necessary detours (See Section IV-B.1 for a detailed example). We augmented the objective function to encourage the simulated pedestrians to move and thus explore new directions to escape from the “freezing state”.

Our POMDP model integrates the improved ORCA. It encodes pedestrian intentions as hidden variables, and applies ORCA in its transition function to predict pedestrian motions according to their intentions and interactions. By solving the intention POMDP, our system performs intention- and interaction-aware planning for a robot vehicle. We use HyP-DESPOT [2], a hybrid parallel online POMDP planning algorithm, to efficiently solve the POMDP model. The algorithm maintains a *belief* i.e., probability distribution, over possible intentions of each pedestrian. At each time step, it performs a lookahead search in a belief tree reachable under future actions and observations, to plan for optimal vehicle control.

Experiments show that the proposed pedestrian motion model better predicts pedestrian motions over prior models. By integrating it into the planning system, our robot vehicle successfully avoids collisions with pedestrians, and achieves its goal more efficiently and smoothly in the tested scenarios.

II. RELATED WORK

A. Planning for Navigation among Pedestrians

Considerable research has been conducted on navigation among pedestrians. Many previous planning algorithms ignore pedestrians’ intentions and interactions when predicting their motions. For example, the approaches in [3], [4] treat pedestrians as static obstacles and handle pedestrian dynamics through online replanning. Other approaches assume simple independent motions for pedestrians, e.g., constant velocity [5]. Another group of planning algorithms consider pedestrians’ intentions, but do not explicitly model their interactions. For example, Foka and Trahanias integrated navigation goals and short-term motions into a dynamic

¹The authors are with School of Computing, National University of Singapore. {yuanfu, caipp, dyhsu, leews}@comp.nus.edu.sg

²The authors are with Department of Computer Science, University of North Carolina at Chapel Hill, USA. {ab, dm}@cs.unc.edu

costmap [6], assuming that pedestrians move independently and do not interact with each other. Thompson, Horiuchi and Kagami [7] followed a very similar approach, using probability grids to encode pedestrians' independent motions. Both [8] and [9] learned pedestrian motion patterns from data to predict trajectories, then applied A* to compute a path for the vehicle using those trajectories. These data-driven approaches, however, can hardly generalize to novel environments [7]. Bai et al. [10] modeled the navigation problem as a POMDP to handle uncertain pedestrian intentions, but still used a simple straight-line motion model for them. Some planning algorithms, though few, have modeled both intentions and interactions of pedestrians. However, they often overlook the underlying uncertainty. The planning in [11] modeled pedestrian-vehicle interactions using interacting Gaussian processes. However, their method assumes each pedestrian has a fixed navigation goal, hence does not capture the uncertainty on pedestrian intentions. Kuderer et al. [12] performed navigation by optimizing trajectories in a joint state space of all pedestrians and the vehicle. It assumes that pedestrians' intentions are fixed in a planning cycle. The method is also highly computationally expensive.

Our work is most related to the intention-aware planning in [10], but our POMDP models both intentions and interactions, and their underlying uncertainty. Instead of assuming straight-line motions of pedestrians as in [10], we integrate a sophisticated pedestrian motion model into the POMDP to better characterize pedestrians' short-term motions.

B. Pedestrian Motion Model

Pedestrian motion modeling has been studied extensively. There are three main categories of pedestrian motion models: social force based, data-driven and geometric approaches. Most existing methods do not explicitly model the interactions between pedestrians and non-holonomic vehicles. Social force models [13], [14], [15] assume that pedestrians are driven by virtual forces that measure the internal motivations of individuals for reaching the goal, avoiding obstacles, or performing certain actions, etc. These approaches perform well in simulating crowds, but often predict the movements of individual pedestrian poorly [12]. Data-driven approaches [16], [17] learn pedestrian dynamics from past trajectories. However, the training data required is often hard to obtain. Besides, the learned models may not generalize well to novel scenarios. Geometric approaches compute collision-free paths for multiple agents via optimization in the feasible geometric space. This category includes the well-known Velocity Obstacle (VO) based [18] and the Reciprocal Velocity Obstacle (RVO) based algorithms [19], [1], [20].

Some previous work have tried to handle non-holonomic motion of vehicles. The method in [21] uses a trajectory tracking controller to generate non-holonomic vehicle motion after applying ORCA. However, inside ORCA, the vehicle is still considered as a holonomic agent. Models in [22], [23] handle pedestrian-vehicle interaction specifically at crosswalks. Hence they are not applicable for other general scenes.

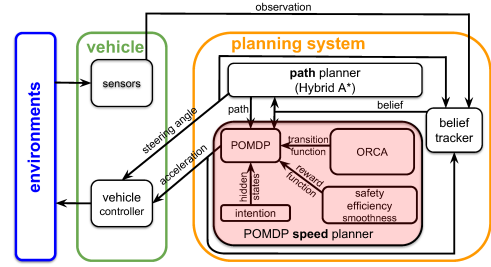


Fig. 1: An overview of our driving system. The region shaded in red presents a detailed view of our speed planner.

Our pedestrian motion model is developed upon ORCA [1], a model based on optimal reciprocal collision avoidance. We improve ORCA by taking the non-holonomic nature of vehicles into account and enhancing its objective function to simulate more natural interactions.

III. OVERVIEW

Fig. 1 shows an overview of our driving system. It consists of a belief tracker, a *path* planner, and a *speed* planner. The belief tracker maintains a belief over pedestrian intentions and constantly updates it to integrate new observations. The path planner uses hybrid A* [24] to plan a non-holonomic driving path, and extracts vehicle steering commands from the path. The speed planner solves an intention POMDP model to control the vehicle speed along the planned path. The planning system re-plans both the steering and the speed at 3 HZ.

This work focuses on building the speed planner to achieve pedestrian intention- and interaction-aware autonomous driving; we refer readers to [10] for more details on the path planner and the belief tracker. The red block in Fig. 1 presents a detailed view of our speed planner. We constructed a POMDP model encoding pedestrian intentions as hidden states. At each time step, the speed planner performs a look-ahead search in a belief tree, using a pedestrian motion model (ORCA) to predict pedestrian behaviors. The vehicle then executes the first action in the plan, which is optimized for safe, efficient and smooth driving among many pedestrians.

We will first introduce our pedestrian motion model in Section IV, and then introduce our POMDP speed planner that integrates this pedestrian motion model in Section V.

IV. PEDESTRIAN MOTION PREDICTION MODEL

The pedestrian motion model takes as input the intentions of pedestrians and the vehicle, and simulates their interactions to predict the motions of pedestrian. We improve ORCA [1], a pedestrian simulation algorithm based on reciprocal collision avoidance, to model more natural pedestrian-vehicle and pedestrian-pedestrian interactions.

For completeness, we will first introduce ORCA and its limitations, and present our model that addresses these issues.

A. Optimal Reciprocal Collision Avoidance

For a given agent, e.g., a pedestrian or a vehicle, ORCA generates a half-plane of velocities that allows it to avoid collision with another agent. It then selects the optimal velocity

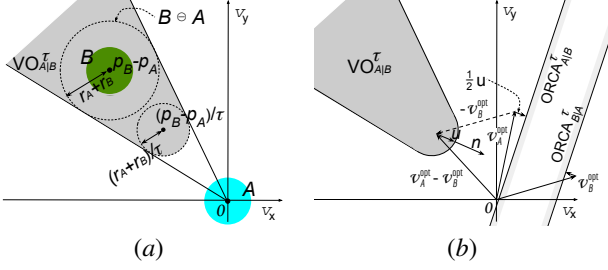


Fig. 2: (a) $VO_{A|B}^\tau$ (gray), the velocity obstacle of agent A (blue) induced by agent B (green) for time τ , is a truncated cone with its apex at the origin (in velocity space) and its legs tangent to the disc $B \oplus A$. If the relative velocity of A with respect to B is in $VO_{A|B}^\tau$, A and B will collide with each other before time τ . (b) $ORCA_{A|B}^\tau$ is a half-plane divided by the line that is perpendicular to the vector u through the point $v_A^{\text{opt}} + \frac{1}{2}u$, where u is the vector from $v_A^{\text{opt}} - v_B^{\text{opt}}$ to the closest point on the boundary of $VO_{A|B}^\tau$.

for the given agent from the intersection of all computed half-planes using linear programming. ORCA computes the half-planes based on Velocity Obstacle (VO) [18].

1) *Velocity Obstacles*: For two agents A and B , the velocity obstacle $VO_{A|B}^\tau$ is defined as the set of all *relative* velocities of A with respect to B that will result in a collision between A and B before time τ . Formally, $VO_{A|B}^\tau$, the *velocity obstacle* of agent A induced by B with time τ is defined as,

$$VO_{A|B}^\tau = \{v | \delta(p_A, v, \tau) \cap (B \oplus A) \neq \emptyset\}. \quad (1)$$

The Minkowski difference $B \oplus A$ inflates the geometry of B by that of A , so that A can be treated as a single point. $\delta(p_A, v, \tau)$ is the straight-line relative trajectory traveled by A with respect to B during time $(0, \tau)$, by starting from its position p_A , and taking the relative velocity v . For simplicity, ORCA assumes all the agents are of disc shape. The Minkowski difference $B \oplus A$ then becomes a disk of radius $r_A + r_B$, where r_A and r_B are the radius of A and B , respectively. Suppose A and B are moving with velocity v_A and v_B , respectively. If $v_A - v_B \notin VO_{A|B}^\tau$, A and B are guaranteed to be collision-free for at least τ time. See Fig. 2a for the geometric interpretation of velocity obstacle.

2) *Collision-Avoiding Velocity Set*: Suppose B selects its velocity from a velocity set V_B , to avoid the collision for at least τ time, A needs to set its velocity to v_A such that $v_A \notin VO_{A|B}^\tau \oplus V_B$, where \oplus denotes the Minkowski sum operation. This leads to the definition of *collision-avoiding velocity set* of A with respect to B :

$$CA_{A|B}^\tau(V_B) = \{v | v \notin VO_{A|B}^\tau \oplus V_B\}. \quad (2)$$

A pair of velocity set V_A and V_B is called *reciprocal collision-avoiding* if $V_A \subseteq CA_{A|B}^\tau(V_B)$ and $V_B \subseteq CA_{B|A}^\tau(V_A)$; it is further called *reciprocal maximal* if $V_A = CA_{A|B}^\tau(V_B)$ and $V_B = CA_{B|A}^\tau(V_A)$.

3) *Optimal Reciprocal Collision-Avoiding Velocity Set*: ORCA attempts to find the pair of reciprocal maximal velocity sets for each pair of agents A and B , with the

guidance of the *optimization velocities* v_A^{opt} for A and v_B^{opt} for B (Fig. 2b), such that the velocity set pair maximizes the amount of permitted velocities close to v_A^{opt} and v_B^{opt} . The optimization velocities v_A^{opt} and v_B^{opt} can be either the preferred velocities of A and B which correspond to their intentions, or simply set as their current velocities. The target pair of velocity sets, denoted as $ORCA_{A|B}^\tau$ for A and $ORCA_{B|A}^\tau$ for B , can be constructed as follows [1].

Suppose that $v_A^{\text{opt}} - v_B^{\text{opt}} \in VO_{A|B}^\tau$, i.e., A and B will collide with each other before time τ by taking these velocities. To achieve collision avoidance with the least effort, ORCA finds a relative velocity from the boundary of $VO_{A|B}^\tau$ that is closest to $v_A^{\text{opt}} - v_B^{\text{opt}}$. Let u be the vector from $v_A^{\text{opt}} - v_B^{\text{opt}}$ to this point.

$$u = (\arg \min_{v \in \partial VO_{A|B}^\tau} \|v - (v_A^{\text{opt}} - v_B^{\text{opt}})\|) - (v_A^{\text{opt}} - v_B^{\text{opt}}). \quad (3)$$

Then u is the smallest change on the relative velocity to avoid the collision within τ time. ORCA lets each agent take half of the responsibilities for collision avoidance, i.e., adapt its velocity by (at least) $\frac{1}{2}u$. It constructs $ORCA_{A|B}^\tau$, the optimal collision-avoiding velocity set of agent A with respect to B , as:

$$ORCA_{A|B}^\tau = \{v | (v - (v_A^{\text{opt}} + \frac{1}{2}u)) \cdot n \geq 0\}, \quad (4)$$

where n is the outward normal at point $(v_A^{\text{opt}} - v_B^{\text{opt}}) + u$ on the boundary of $VO_{A|B}^\tau$. $ORCA_{B|A}^\tau$ is constructed symmetrically (Fig. 2b).

Geometrically, $ORCA_{A|B}^\tau$ and $ORCA_{B|A}^\tau$ are half-planes of velocities in the velocity space (Fig. 2b).

4) *Computing New Velocity*: For an agent A , ORCA computes for each other agent B the optimal reciprocal collision-avoiding velocity set $ORCA_{A|B}^\tau$. The permitted velocity set for A , denoted as $ORCA_A^\tau$, is the intersection of the half-planes $ORCA_{A|B}^\tau$ induced by all B 's:

$$ORCA_A^\tau = \bigcap_{B \neq A} ORCA_{A|B}^\tau. \quad (5)$$

The agent A then selects a new velocity v_A^{new} that is closest to its preferred velocity v_A^{pref} from $ORCA_A^\tau$, i.e.,

$$v_A^{\text{new}} = \arg \min_{v \in ORCA_A^\tau} \|v - v_A^{\text{pref}}\|. \quad (6)$$

The computation of v_A^{new} can be efficiently done using linear programming [1].

B. Remaining Problems in ORCA

The original ORCA has two remaining problems: the *freezing pedestrian problem* and the *violation of non-holonomic constraints* problem.

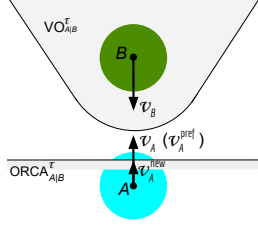


Fig. 3: An example showing the freezing pedestrian problem. Two pedestrians (A and B) are walking towards each other, with velocities v_A and v_B , respectively. Suppose $v_A^{\text{pref}} = v_A$. The new velocity v_A^{new} computed by ORCA is as shown. Its magnitude is much smaller than that of v_A^{pref} , which means A slows down a lot. This behavior is different from that of human. Human usually maintains a similar speed (magnitude) and makes a detour to avoid collisions instead of slowing down a lot.

1) *Freezing Pedestrian Problem*: The objective function (6) for Ori-ORCA attempts to minimize the distance to the pedestrian's preferred velocity which points to his/her goal position, under the collision avoidance constraints. This sometimes causes the “freezing pedestrian problem” when it is used to model pedestrians' motions. Pedestrians will be greedy in walking in their goal directions, which causes pedestrian to walk very slowly or even stay stationary when obstacles block their way to their goals. Pedestrians in reality, however, would like to maintain his/her speed (the magnitude of the velocity) and make detours to bypass the obstacles in such scenarios. See Fig. 3 for an example of this problem.

2) *Violation of Non-holonomic Constraints*: ORCA assumes the motions of agents are holonomic and agents can flexibly change their moving directions to avoid collisions. It is true for pedestrians. Most vehicles in reality, however, are under the non-holonomic kinematic constraints and cannot freely change their directions. With the holonomic assumption, pedestrians in ORCA will have wrong anticipations on the vehicle's reactions during reciprocal collision avoidance. This often leads to unnatural motion predictions for pedestrians. For example, in ORCA, when a pedestrian is close to a vehicle, he/she still thinks that the vehicle can flexibly avoid him/her by moving side-wise, thus will not change his/her velocity much. In reality, a pedestrian in this dangerous situation would try his/her best to avoid collisions.

C. New-ORCA for Autonomous Driving

In this section, we present our improved ORCA which addresses the aforementioned problems. We use Ori-ORCA to refer the original ORCA and New-ORCA to refer our improved ORCA.

1) *Objective Function with Patience*: The freezing pedestrian problem could be addressed by several approaches, such as performing multiple-step lookahead in ORCA, or applying a global planner to replan a preferred velocity for each pedestrian. However, these approaches would significantly increase the computation time of ORCA, and are thus not suitable for our application, because ORCA will be used

heavily during each planning cycle. In this section, we propose a solution to the freezing pedestrian problem that has rather low computational overhead.

Concretely, we design a new objective function for ORCA as follows

$$v_A^{\text{new}} = \arg \min_{v \in \text{ORCA}_A^\tau} \left\{ \|v - v^{\text{pref}}\|^2 + \frac{1}{\varrho_A} \left| \|v\|^2 - \|v^{\text{pref}}\|^2 \right| \right\}, \quad (7)$$

where $\varrho_A \in (0, 1]$ is a variable measuring the *patience* of a pedestrian A . We observed that, people usually prefer to maintain their current speed, and often get more and more impatient when staying stationary or moving very slowly if their intentions are not staying put. Therefore, we introduce the second term in (7) to penalize slowing down of pedestrians. We further use the pedestrian's *patience* level ϱ to control the strength of this penalization. Intuitively, if a pedestrian walks with a low speed, it gets more and more impatient (ϱ decreases) as time goes. The weight $\frac{1}{\varrho}$ for the second term in (7) then increases and encourages the pedestrian to explore alternative directions that enable him/her to move faster.

We set the patience for each pedestrian whose intention is not staying put as follows. It is set to 1 initially and starts to decrease exponentially with the time if the pedestrian's new speed is less than some threshold ς . We set ς to $0.2\|v^{\text{pref}}\|$ in practice. When the patience is smaller than ϱ_{\min} ($\varrho_{\min} = 0.1$ in our experiments), we set it to ϱ_{\min} ; it is reset to 1 once the new speed is no longer smaller than ς . Empirically, we suggest to set $\varsigma \in (0, 0.3\|v^{\text{pref}}\|)$ and $\varrho_{\min} \in (0.05, 0.15)$. For pedestrians with intentions of staying put, we set their patiences always to 1.

People may concern that the objective function (7) is no longer convex when $\varrho < 1$ and that increases the computation cost. From our observation, fortunately, pedestrian velocities are larger than ς in most of the time, which guarantees ϱ to be 1 for most pedestrians in most of the time. Hence we can still solve New-ORCA very efficiently.

2) *ORCA with Changing Responsibilities*: To handle the non-holonomic motion of the vehicle and further produce more natural pedestrian-vehicle interactions, we let pedestrians take more responsibilities for reciprocal collision avoidance when they are very close to a vehicle. The vehicle takes less responsibilities accordingly. The responsibility $r \in (0, 1)$ of an agent is defined as the ratio of the velocity u (defined in (3)) this agent takes to avoid the collision. If an agent A takes r responsibility to avoid the collision with B , its $\text{ORCA}_{A|B}^\tau$ will be computed as,

$$\text{ORCA}_{A|B}^\tau = \{v | (v - (v_A^{\text{opt}} + ru)) \cdot n \geq 0\},$$

and B will compute its $\text{ORCA}_{B|A}^\tau$ with the responsibility $1 - r$ accordingly. On one hand, this mechanism selects for the vehicle velocities that are closer to their current velocity, which better complies with the non-holonomic constraints. On the other hand, it models pedestrians' urgency to avoid collisions with the non-holonomic vehicle.

Initially, the pedestrian and the vehicle each take half of the responsibilities. When their distance is within some

threshold d , the responsibility of the pedestrian increases linearly as he/she approaches the vehicle. The responsibility reaches a maximum value R when the distance decreases to zero. We set $d = 1.5$ and $R = 0.95$ in our experiments. We found empirically that the linear function works well.

V. POMDP PLANNING FOR INTENTION AND INTERACTION- AWARE AUTONOMOUS DRIVING

Our planning system uses a two-level hierarchical approach [10] for autonomous driving to reduce the computational cost. At the high level, hybrid A* [24] is used to plan a path; at the low level, a POMDP model is built to control the vehicle *speed* along the planned path. This section focuses on the low-level POMDP speed planner.

A. POMDP Preliminaries

Formally, a POMDP is defined as a tuple (S, A, Z, T, O, R, b_0) , where S , A and Z represents the state space, the action space and the observation space, respectively. The transition function $T(s, a, s') = p(s'|s, a)$ models the imperfect robot control and environment dynamics. It defines the probability of transiting to a state s' from a state s , after the robot executing an action a . The observation function $O(s, a, z) = p(z|a, s)$ characterizes the robot's sensing noises. It defines the probability of receiving the observation z after the robot executes a and reaches s . The reward function $R(s, a)$ defines a real-valued immediate reward for executing a at s . Due to imperfect sensing, the robot does not know the exact state of the world. It maintains a *belief*, a probability distribution over S , and reasons over the space of beliefs. At each time step, the belief is updated via the Bayes' rule:

$$b_t(s') = \eta O(s', a_t, z_t) \sum_{s \in S} T(s, a_t, s') b_{t-1}(s), \quad (8)$$

where η is a normalizing constant.

POMDP planning aims to find a *policy* π , a mapping from a belief b to an action a , that maximizes the expected total discounted rewards with initial belief $b_0 = b$:

$$V_\pi(b) = \mathbb{E} \left(\sum_{t=0}^{\infty} \gamma^t R(s_t, \pi(b_t)) \mid b_0 = b \right), \quad (9)$$

where s_t is the state at time t , $\pi(b_t)$ is the action that the policy π chooses at time t , and $\gamma \in (0, 1)$ is a discount factor that places preferences for immediate rewards over future ones. The expectation is taken over the sequence of uncertain state transitions and observations over time.

POMDP planning is usually performed as a lookahead search in a *belief tree*. Each node of the belief tree corresponds to a belief. At each node, the tree branches on all actions and observations. Beliefs in child node are computed using the Bayes' rule (8). The output of the search is an optimal policy conditioned on the initial belief.

B. Intention POMDP Model for Autonomous Driving

1) *State Modeling*: A state in our model consists of two parts: the vehicle state and the pedestrian state. The vehicle state consists of its 2D position (x, y) , its heading direction θ , and its instantaneous speed v . The state of a pedestrian consists of the position (x, y) , speed v and intention g of the pedestrian. The intention of a pedestrian is represented as his/her goal location in the environment. Pedestrians' intentions are hidden variables and must be inferred from observations over time.

2) *Action Modeling*: Our model uses discrete actions: at each time step, the planning can choose to ACCELERATE, DECELERATE, or MAINTAIN the current vehicle speed, in order to avoid collisions and navigate efficiently and smoothly towards the goal.

3) *Observation Modeling*: An observation in our model consists of the vehicle position, its speed, and the positions of all pedestrians. Compared to pedestrians' hidden intentions, these observations are relatively accurate and their noises will not have a significant affect on decision making. Therefore, we assume them to be fully observable, and focus more on modeling the uncertainty in pedestrians' intentions, which is not directly observable. The POMDP planning infers those intentions from a history of observation over time.

4) *Transition (Intention and Interaction) Modeling*: We decompose the transition function into vehicle transition and pedestrian transitions.

In each transition step, the vehicle takes a discrete action, and drives for a fixed time duration Δt along the path planned by hybrid A*. We add a small noise to the transition to model imperfect control. The resulting vehicle transition function, denoted as $p(x_{t+1}, y_{t+1}, v_{t+1} | x_t, y_t, v_t, a)$, satisfies the non-holonomic constraints.

Pedestrians' transitions are calculated using New-ORCA. Given a set of intentions, (g^1, g^2, \dots, g^n) , of n surrounding pedestrians, we compute for each pedestrian a preferred velocity, pointing to his/her goal with the speed assumed to be roughly the human-walking speed, $1.2m/s$. These preferred velocities, together with positions of pedestrians and the vehicle, are input to New-ORCA to compute new velocities and predict next-step positions of pedestrians. To model stationary pedestrians, a "stop intention" (with preferred velocity 0) is also included. Gaussian noises are added on those predicted positions to model uncertainty in pedestrian-vehicle and pedestrian-pedestrian interactions. This pedestrian transition model is denoted as:

$$p(x_{t+1}^1, y_{t+1}^1, \dots, x_{t+1}^n, y_{t+1}^n | x_t^1, y_t^1, \dots, x_t^n, y_t^n, g^1, \dots, g^n, x_t, y_t, v_t) \quad (10)$$

This pedestrian transition function (10) is conditioned on a set of given pedestrian intentions. Uncertainty in their intentions is systematically handled by the belief tree search and belief update in our POMDP planning.

5) *Reward Modeling*: The reward function encourages the vehicle to drive safely, efficiently, and smoothly. For safety, we give a huge penalty $R_{col} = -1000 \times (v^2 + 0.5)$ to the



Fig. 4: (a) Pedestrian video. (b) Predicted trajectories using different motion models, compared with ground truth.

TABLE I: Comparison of the rate of successful trajectory predictions for different motion models.

Model	Const-Vel	Pref-Vel	Ori-ORCA	New-ORCA
Successful Rate	0.521	0.674	0.760	0.804

robot if it collides with any pedestrian, with speed v . For efficiency, we assign a reward $R_{\text{goal}} = 0$ to the vehicle when it reaches the goal, and assign a penalty $R_{\text{speed}} = \frac{v - v_{\text{max}}}{v_{\text{max}}}$ to encourage the vehicle to choose a current speed v closer to its maximum speed v_{max} , when it is safe to do so. For smoothness of the drive, we add a small penalty $R_{\text{acc}} = -0.1$ for choosing the action ACCELERATE and DECELERATE, to penalize the excessive speed changes.

C. HyP-DESPOT

We use HyP-DESPOT [2] to efficiently solve the intention POMDP. HyP-DESPOT performs parallel online POMDP planning through CPU-based parallel belief tree search and GPU-based parallel Monte Carlo simulations at leaf nodes of the belief tree. Within a simulation step in the planning, HyP-DESPOT can further parallelize the transitions of individual pedestrians. Benefiting from its computational efficiency, our planning system is able to re-plan the vehicle speed at 3Hz.

VI. EXPERIMENTS

In the experiments, we first evaluate the prediction accuracy of our pedestrian motion model using real-world data. Then, we illustrate the performance of our planning system on three challenging scenarios in simulation. Finally, we show that our planning system can successfully drive a real robot vehicle among pedestrians.

A. Pedestrian Motion Predictions on Real-world Data

To test the prediction accuracy, we extracted 2D trajectories from real-world pedestrian videos shot in a campus plaza (Fig. 4a), and compared the predicted trajectories with them. Ground truth positions of pedestrians are obtained by manually labeling 46 trajectories, each for a particular pedestrian. Concretely, we apply our model to predict a trajectory, which consists of a discretized sequence of positions, for a duration of 3 seconds. Each position in the trajectory corresponds to one time frame. The duration between two adjacent frames is 0.33 second. We compute the distance between the predicted position at each frame and the ground truth at the same frame. The prediction is counted as a success if the average

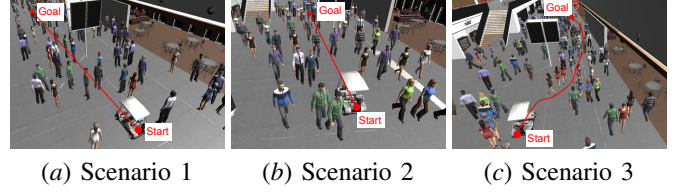


Fig. 5: Three designed scenarios for autonomous driving in a crowd. The vehicle is required to drive from the Start position to the Goal position. The performance for different algorithms under each scenario is presented in TABLE II.

distance over all frames is less than d meters. We set $d = 0.4$ to have the average one-second error smaller than 1.2 meters, roughly the stride length of a pedestrian.

We compared our success rate with those of other motion models: constant velocity (Const-Vel), preferred velocity (Pref-Vel), and the original ORCA (Ori-ORCA). Const-Vel assumes each pedestrian keeps his/her current velocity; Pref-Vel assumes each pedestrian walks towards his/her goal at a constant speed. Since Pref-Vel, Ori-ORCA and New-ORCA all require goal information to predict pedestrian motions, we extract the ground truth goal from the trajectory and use it in all the models for a fair comparison. Results in TABLE I shows that our model achieves higher success rate than all baselines.

For a detailed view of the performance, we selected an example scene and visualized the predictions and the ground truth in Fig. 4b. In this scene, a pedestrian walking towards GOAL is blocked by a moving vehicle. Both Const-Vel and Pref-Vel predict that the pedestrian will walk in a straight line, ignoring that such trajectories lead to collisions. Both Ori-ORCA and New-ORCA predict that the pedestrian will detour. However, only our model successfully predicts that the pedestrian will maintain his speed during the detour.

B. Autonomous Driving in Simulation

We analyze the performance of our planning algorithm (POMDP-New-ORCA) by comparing it with two types of baselines. The first type includes constant speed (Const-Speed), reactive controller (Reactive-Controller), and the POMDP speed planner with Pref-Vel model (POMDP-Pref-Vel). They only control the speed, and rely on hybrid A* to generate steering commands. The other type includes dynamic hybrid A* (Dynamic-Hybrid-A*), which controls both the steering and the speed. All the baselines do not model at least one of the following key aspects: intentions, interactions, and uncertainty. By comparing our algorithm with these baselines, we analyzed the benefit of modeling these aspects. Now we describe these baselines in detail.

Const-Speed drives the vehicle at a constant speed. We set the speed as the average speed of POMDP-New-ORCA, to compare the safety when it achieves the same efficiency as our algorithm. Reactive-Controller avoids collisions with pedestrians without modeling intentions and interactions. It compares D , the distance to the nearest pedestrian, with two distance thresholds D_{far} and D_{near} , and then chooses

TABLE II: Performance Comparison for the three scenarios. For each scenario, we run for 300 times. The avg. collision rate, avg. travel time and avg. number of accelerations and decelerations are all calculated using only the successful trials.

Scenarios	Algorithm	Collision Rate	Travel Time (s)	Accel/Decel number	Success Rate
Scenario 1	Const-Speed	0.177	24.19	0	1.0
	Reactive-Controller	-	-	-	0.0
	POMDP-Pref-Vel	0.0	27.27	46.6	0.97
	POMDP-New-ORCA	0.0	24.19	45.1	1.0
Scenario 2	Const-Speed	0.0633	34.63	0	1.0
	Reactive-Controller	0.0	75.72	128.0	1.0
	POMDP-Pref-Vel	0.0	62.57	141.4	0.977
	POMDP-New-ORCA	0.0	34.63	104.8	1.0
Scenario 3	Const-Speed	0.033	71.38	0	1.0
	Dynamic-Hybrid-A*	0.023	50.46	36.1	1.0
	Reactive-Controller	0.0	183.11	128.8	0.817
	POMDP-Pref-Vel	0.0	105.20	190.7	0.91
	POMDP-New-ORCA	0.0	74.36	157.6	0.963

DECELERATE if $D < D_{\text{near}}$, ACCELERATE if $D > D_{\text{far}}$, or MAINTAIN if $D_{\text{near}} < D < D_{\text{far}}$. POMDP-Pref-Vel is similar to our algorithm, except that it uses Pref-Vel instead of New-ORCA as the pedestrian motion model, considering only intentions. Dynamic-Hybrid-A* is hybrid A* augmented with an acceleration dimension in the search space and with predicted pedestrian positions in the collision checking module. Pedestrian motions are predicted using a constant velocity model. Dynamic-Hybrid-A* also does not explicitly model intentions and interactions.

The criteria for comparison include safety, efficiency and smoothness. We measure the safety by the collision rate, the efficiency by the success rate and the travel time, and the smoothness by the number of accelerations and decelerations. We ran 300 trials for each scenario and computed the success rate; a trial is considered as successful if the vehicle achieves its goal within 6 minutes. We computed the average collision rate, travel time and accel/decel number *using only the successful trials*.

We tested the algorithms in three simulated scenarios (Fig. 5). In the first two scenarios, modeling intentions and interactions are especially important. All pedestrians in Scenario 1 (Fig. 5a) stay stationary. In Scenario 2 (Fig. 5b), all pedestrians keep walking towards the vehicle. In both scenarios, the vehicle is required to drive along a *straight line* for 16 meters. Scenario 3 (Fig. 5c) represents a more common scene in real life. It contains 150 pedestrians walking towards one of the seven goals. The vehicle is required to drive from one end of the hall to the other, with no restriction on the path.

We built our simulator with the Unity game engine, and implemented a package of sensors, including 2D LIDARs, wheel encoders, etc. The simulator uses New-ORCA to simulate pedestrian motions. The simulator communicates with our planning system using the Robot Operation System (ROS). Note that though this simulator is designed for testing our planning system, it is general and can be used in other autonomous driving applications involving pedestrians.

TABLE II shows the performance of the tested algorithms. Overall, our algorithm, POMDP-New-ORCA, guarantees safety, while Const-Speed and Dynamic-Hybrid-A* result in



Fig. 6: (a) The system overview of the robot vehicle. (b) The robot vehicle drives among pedestrians on a campus plaza.

collisions, and it outperforms the other baselines that also achieve safety, Reactive-Controller and POMDP-Pref-Vel, in efficiency and smoothness.

Const-Speed drives the vehicle aggressively in all three scenarios; this leads to collisions when pedestrians fail to avoid the vehicle. Dynamic-Hybrid-A* also causes collisions. Without modeling intentions and interactions, it fails to accurately predict pedestrian motions. Moreover, since no uncertainty is considered, it drives the vehicle aggressively. Reactive-Controller drives the vehicle over-conservatively in all scenarios because it does not model the interactions of reciprocal collision avoidance. For example, in Scenario 1, Reactive-Controller keeps the vehicle waiting for stationary pedestrians in front, in order to guarantee safety. Hence the vehicle never reaches the goal (0 success rate). With our algorithm, the vehicle knows that pedestrians will cooperate with it to avoid collisions. Therefore, instead of waiting, the vehicle slowly moves forward to convey its intention. Pedestrians hence give way to the vehicle. POMDP-Pref-Vel can achieve relatively higher success rates than Reactive-Controller, but still requires much more travel time and drives less smoothly than our algorithm.

C. Autonomous Driving on A Real Robot

We further tested the performance of our planning system on a real robot vehicle (Fig. 6a).

The sensor package of our robot vehicle mainly includes

two LIDARs, an Inertial Measurement Unit (IMU), and wheel encoders. The top-mounted SICK LMS151 LIDAR and the bottom-mounted SICK TiM551 LIDAR are used for pedestrian detection and localization, respectively. Our planning system runs on an Ethernet-connected laptop with an Intel Core i7-4770R CPU running at 3.90 GHz, a GeForce GTX 1050M GPU, and 16 GB main memory. The maximum speed for the vehicle is set to 1m/s for safety. The planning system is implemented on ROS. Our vehicle detects pedestrians from laser points using K -means clustering, and tracks pedestrians between two adjacent time frames by comparing the difference of their corresponding laser clusters. It localizes itself in a given map using adaptive Monte Carlo localization [25], which integrates the LIDAR data, IMU data, and wheel encoder data.

We tested our autonomous driving system on a campus plaza (Fig. 6b) for multiple times. Overall, our planning system performs well. The vehicle achieved its goal efficiently, smoothly and avoidance the pedestrians successfully in all trials. See the video at <https://www.dropbox.com/s/45ay8tt73f02u6c/ad.mp4?dl=0> for more details.

VII. CONCLUSION AND FUTURE WORK

We developed an online planning system for autonomous driving in a crowd that considers both intentions and interactions of pedestrians. Our planning system combines a pedestrian motion model and a POMDP algorithm seamlessly to plan optimal vehicle actions under the uncertainty in pedestrian intentions and interactions. Our pedestrian motion model improves over previous models on the accuracy of predicting pedestrian interactions in the presence of the vehicle. By utilizing this prediction model, our planning system enables robot vehicles to drive safely, efficiently and smoothly among many pedestrians.

There are multiple directions we can work on in the future. First, we plan to better incorporate the non-holonomic constraints of vehicles into the computation of ORCA velocity sets, instead of using only changing responsibilities. Second, we can apply more sophisticated pedestrian motion models, such as GLMP [26], to improve the simulator. Finally, our POMDP model is actually a *POMDP-lite* [27], a subclass of POMDPs where the hidden state variables are constant or only change deterministically. Our POMDP model can be potentially solved more efficiently using POMDP-lite.

REFERENCES

- [1] J. Van Den Berg, S. Guy, M. Lin, and D. Manocha, "Reciprocal n-body collision avoidance," *Robotics Research - The 14th Int. Symposium*, pp. 3–19, 2011.
- [2] P. Cai, Y. Luo, D. Hsu, and W. S. Lee, "HyP-DESPOT: A hybrid parallel algorithm for online planning under uncertainty," *arXiv preprint arXiv:1802.06215*, 2018.
- [3] W. Burgard, A. B. Cremers, D. Fox, D. Hähnel, G. Lakemeyer, D. Schulz, W. Steiner, and S. Thrun, "The interactive museum tour-guide robot," in *Proc. of the 15th National Conference on Artificial Intelligence and 10th Innovative Applications of Artificial Intelligence Conf.*, pp. 11–18, 1998.
- [4] A. Bauer, K. Klasing, G. Lidoris, Q. Mühlbauer, F. Rohrmüller, S. Sosnowski, T. Xu, K. Kühnlenz, D. Wollherr, and M. Buss, "The autonomous city explorer: Towards natural human-robot interaction in urban environments," *Int. J. of Social Robotics*, vol. 1, no. 2, pp. 127–140, 2009.
- [5] R. Kümmerle, M. Ruhnke, B. Steder, C. Stachniss, and W. Burgard, "Autonomous robot navigation in highly populated pedestrian zones," *J. of Field Robotics*, vol. 32, no. 4, pp. 565–589, 2015.
- [6] A. F. Foka and P. E. Trahanias, "Predictive autonomous robot navigation," in *Proc. IEEE/RSJ Int. Conf. on Intelligent Robots & Systems*, vol. 1, pp. 490–495, IEEE, 2002.
- [7] S. Thompson, T. Horiuchi, and S. Kagami, "A probabilistic model of human motion and navigation intent for mobile robot path planning," in *Proc. of the 4th ICARA*, pp. 663–668, IEEE, 2009.
- [8] F. Large, D. A. V. Govea, T. Fraichard, and C. Laugier, "Avoiding cars and pedestrians using v-obstacles and motion prediction," in *Proc. of the IEEE Intelligent Vehicle Symp.*, 2004.
- [9] M. Bennewitz, W. Burgard, G. Cielniak, and S. Thrun, "Learning motion patterns of people for compliant robot motion," *Int. J. Robotics Research*, vol. 24, no. 1, pp. 31–48, 2005.
- [10] H. Bai, S. Cai, N. Ye, D. Hsu, and W. S. Lee, "Intention-aware online POMDP planning for autonomous driving in a crowd," in *Proc. IEEE Int. Conf. on Robotics & Automation*, pp. 454–460, IEEE, 2015.
- [11] P. Trautman and A. Krause, "Unfreezing the robot: Navigation in dense, interacting crowds," in *Proc. IEEE/RSJ Int. Conf. on Intelligent Robots & Systems*, pp. 797–803, IEEE, 2010.
- [12] M. Kuderer, H. Kretzschmar, C. Sprunk, and W. Burgard, "Feature-based prediction of trajectories for socially compliant navigation," in *Proc. Robotics: Science & Systems*, 2012.
- [13] D. Helbing and P. Molnar, "Social force model for pedestrian dynamics," *24th SIBGRAPI Conf. on Graphics, Patterns and Images*, vol. 51, no. 5, p. 4282, 1995.
- [14] R. Löhner, "On the modeling of pedestrian motion," *Applied Mathematical Modelling*, vol. 34, no. 2, pp. 366–382, 2010.
- [15] G. Ferrer, A. Garrell, and A. Sanfeliu, "Robot companion: A social-force based approach with human awareness-navigation in crowded environments," in *Proc. IEEE/RSJ Int. Conf. on Intelligent Robots & Systems*, pp. 1688–1694, IEEE, 2013.
- [16] Y. Chen, M. Liu, S.-Y. Liu, J. Miller, and J. P. How, "Predictive modeling of pedestrian motion patterns with bayesian nonparametrics," in *AIAA Guidance, Navigation, and Control Conf.*, p. 1861, 2016.
- [17] C. Zhou, B. Balle, and J. Pineau, "Learning time series models for pedestrian motion prediction," in *Proc. IEEE Int. Conf. on Robotics & Automation*, pp. 3323–3330, IEEE, 2016.
- [18] P. Fiorini and Z. Shiller, "Motion planning in dynamic environments using velocity obstacles," *Int. J. Robotics Research*, vol. 17, no. 7, pp. 760–772, 1998.
- [19] J. Van den Berg, M. Lin, and D. Manocha, "Reciprocal velocity obstacles for real-time multi-agent navigation," in *Proc. IEEE Int. Conf. on Robotics & Automation*, pp. 1928–1935, IEEE, 2008.
- [20] J. Snape, J. Van Den Berg, S. J. Guy, and D. Manocha, "The hybrid reciprocal velocity obstacle," *IEEE Transactions on Robotics*, vol. 27, no. 4, pp. 696–706, 2011.
- [21] J. Alonso-Mora, A. Breitenmoser, P. Beardsley, and R. Siegwart, "Reciprocal collision avoidance for multiple car-like robots," in *Proc. IEEE Int. Conf. on Robotics & Automation*, pp. 360–366, IEEE, 2012.
- [22] M. Liu, W. Zeng, P. Chen, and X. Wu, "A microscopic simulation model for pedestrian-pedestrian and pedestrian-vehicle interactions at crosswalks," *PLoS one*, vol. 12, no. 7, p. e0180992, 2017.
- [23] A. Gorrini, G. Vizzari, and S. Bandini, "Towards modelling pedestrian-vehicle interactions: Empirical study on urban unsignalized intersection," *arXiv preprint arXiv:1610.07892*, 2016.
- [24] T. S. Stanley, "The robot that won the darpa grand challenge: research articles," *Journal Robotics System*, vol. 23, no. 9, pp. 661–692, 2006.
- [25] S. Thrun, W. Burgard, and D. Fox, *Probabilistic robotics*. MIT press, 2005.
- [26] A. Bera, S. Kim, T. Randhavane, S. Pratapa, and D. Manocha, "GLMP-realtime pedestrian path prediction using global and local movement patterns," in *Proc. IEEE Int. Conf. on Robotics & Automation*, pp. 5528–5535, IEEE, 2016.
- [27] M. Chen, E. Frazzoli, D. Hsu, and W. S. Lee, "POMDP-lite for robust robot planning under uncertainty," in *Proc. IEEE Int. Conf. on Robotics & Automation*, pp. 5427–5433, IEEE, 2016.